JOURNAL OF AIRCRAFT
Vol. 39, No. 2, March–April 2002

Effect of Microlift Force on the Performance of Ultralight Aircraft

Nicola de Divitiis*
University of Rome "La Sapienza," 00184 Rome, Italy

Microlift force, which is the aerodynamic force developed in the presence of a wind gradient, can be responsible for a sizeable improvement of gliding performance of ultralight aircraft. A mathematical formulation based on Lagrange's equation method for the analysis of microlift is presented, where the effects of vertical velocity gradients on aircraft motion are taken into account. After giving some details on the modeled vehicle, the behavior of an ultralight sailplane during flight in a wind gradient is investigated. Optimal maneuvers are computed to interpret and discuss the performance of ultralight sailplanes soaring in a wind gradient. The proposed approach provides an effective means for understanding and improving the piloting techniques for sailplane and ultralight aircraft in nonuniform wind.

Nomenclature

A_g	=	gust speed
AR	=	aspect ratio
b	=	wing span
C_D	=	drag coefficient
C_L	=	lift coefficient
C_{L_m}	=	microlift coefficient
C_{L_α}	=	lift curve slope
C_l, C_m, C_n	=	aerodynamic moment coefficients in body axes
C_x, C_y, C_z	=	aerodynamic force coefficients in body axes
c	=	mean wing chord
E	=	$mgh + \frac{1}{2}mV^2 + \frac{1}{2}\boldsymbol{\omega}\cdot\boldsymbol{J}\boldsymbol{\omega}$
$\boldsymbol{F}$	=	(X, Y, Z) aerodynamic force in body axes
$\boldsymbol{F}_m$	=	microlift force
$\boldsymbol{G}$	=	reduced wind gradient
$\boldsymbol{g}$	=	gravity acceleration
H	=	space scale of gust
h	=	altitude
h_t	=	E/mg, energy altitude
$\boldsymbol{J}$	=	inertia tensor
$\boldsymbol{L}$	=	transformation matrix from inertial to body frame
l	=	glider length
$\boldsymbol{M}$	=	$[(M_{ij})]$, apparent-mass tensor
M_A	=	$\Sigma_i M_{ii}$, virtual mass
m	=	glider mass
$\boldsymbol{n}$	=	unit vector normal to local wing surface
n_z	=	normal load factor
$\boldsymbol{Q}^e$	=	external moment with respect to c.g.
$\boldsymbol{R}^{-1}$	=	transformation matrix from $\boldsymbol{\omega}$ to $\boldsymbol{\Phi}$
$\boldsymbol{r}$	=	(x, y, z), aircraft position in Earth axes
S	=	wing area
s	=	coordinate along which $\boldsymbol{w}_g$ changes
T	=	kinetic energy of the stream flow
u, v, w	=	inertial velocity in Earth axes
V	=	velocity modulus
$\boldsymbol{v}$	=	inertial velocity in body axes
$\hat{\boldsymbol{v}}$	=	$(\boldsymbol{v} - \boldsymbol{L}\boldsymbol{w}_g)/\lvert\boldsymbol{v} - \boldsymbol{L}\boldsymbol{w}_g\rvert$ relative velocity unit vector
W	=	weight
$\boldsymbol{w}_g$	=	(u_g, v_g, w_g), wind velocity
x, y, z	=	Earth-fixed coordinates
x_B, y_B, z_B	=	body axes coordinates
α, β	=	angle of attack and sideslip, respectively
$\delta(s, \bar{s})$	=	Dirac's delta distribution
$\delta_e, \delta_a, \delta_r$	=	elevator, ailerons, and rudder angles, respectively
ρ	=	air density
$\boldsymbol{\Phi}$	=	$(\varphi, \vartheta, \psi)$ Euler's angles vector
ϕ	=	velocity potential
φ, ϑ, ψ	=	Euler's angles
$\boldsymbol{\omega}$	=	(p, q, r), angular velocity vector in body axes
$\tilde{\boldsymbol{\omega}}$	=	angular velocity in body axes
$\nabla\boldsymbol{w}_g$	=	wind gradient in Earth axes

Introduction

AMONG sailplane piloting techniques, the so-called cross-country flight, which consists of a motion through regions where vertical gusts are present, can be carried out in different fashion depending on wind gradient characteristics and wind loading.

A conventional sailplane in cross-country flight will adopt a conventional soaring technique, where the effect of wind velocity on the angle of attack determines an increase of lift force that in turn allows the aircraft to gain altitude.

When a low wing-loading sailplane flying in a wind gradient is considered, significant improvement of the gliding performance, which is not always recognized among sailplane pilots and consists of two essential aspects related to speed and attitude variations, is observed. The presence of the wind gradient produces the so-called microlift force, generally negligible in conventional aircraft, that allows an ultralight to remain in air much longer than one could expect on the basis of steady-state aerodynamics. In fact, such a force, in the presence of a low wing-loading, causes a sizeable influence on the motion and performance of the vehicle.

The present work is concerned with the development of a method that allows the evaluation of the microlift force and a detailed performance analysis for ultralight sailplanes flying in a nonuniform wind. To this end, it is necessary to provide the definition of microlift force, which is given as follows. A wing in a steady rectilinear flight, moving in a nonuniform gust, develops a lift different from that calculated for zero wind gradient. The microlift is here defined as the part of aerodynamic force, perpendicular to relative velocity $\boldsymbol{v} - \boldsymbol{L}\boldsymbol{w}_g$, given as the difference between the lift developed in the presence of a nonuniform gust and that calculated for zero wind gradient.

Although in the literature it is possible to find some references about the influence of nonuniform wind velocity distributions on the aerodynamic force exerted on a vehicle, to the author's knowledge the effects of microlift force on aircraft motion and related piloting techniques have not received proper attention.

Stojkovic[1] chooses the noninertial wind coordinate system as reference frame, where the sailplane motion is defined and describes the

Received 26 January 2001; revision received 9 November 2001; accepted for publication 11 November 2001.

*Research Fellow, Department of Mechanics and Aeronautics, via Eudossiana, 18.

effects of the wind gradient $\partial w_g/\partial s$ through kinematic considerations related to the time variation of velocity components in the wind gradient. Then, he defines the vertical acceleration as $(\partial w_g/\partial s)V$ and states that the force which occurs in the presence of the wind gradient is given by $m(\partial w_g/\partial s)V$. This assumption, which does not take into consideration the motion of fluid mass about the vehicle, has the consequence that the work done by the so calculated force is, in general, depending upon the reference frame.[1]

In a more general context the force exerted by the fluid on a moving rigid body has been studied by many authors. Lamb[2] uses the expression of the kinetic energy obtained from the potential flows theory and the Lagrange equations to calculate forces and moments acting on a nonlifting body in a stream.

When lifting bodies are dealt with, reference can be made to the so-called linear field approximation proposed by Etkin.[3] The aerodynamic forces and moments caused by a wind gradient are evaluated as caused by an apparent angular velocity $\boldsymbol{\omega}_g \equiv (p_g, q_g, r_g) = \nabla \boldsymbol{w}_g - \nabla^T \boldsymbol{w}_g$. Accordingly, for an aircraft in steady straight flight, the lift variation caused by wind gradient is $\Delta C_L = (\partial C_L/\partial q)(\partial w_g/\partial x_B)$, where $\partial C_L/\partial q$ is a constant aerodynamic derivative. The rotary derivative $\partial C_L/\partial q$ depends upon the c.g. location, whereas, from a physical point of view, the effect of the wind gradient on the aerodynamic force coefficients cannot be influenced by c.g. position. Furthermore use of angular velocity components to represent wind gradients is somewhat limited by vehicle geometry[4] because the vertical dimension of the sailplane is small compared to longitudinal length and wing span, whereas the rotary derivatives are mainly related to changes of the angle of attack on the tail and along the wing span, that is, the result of x and y gradients. Therefore, wind component variations with respect to z are not taken into consideration so that

$$(p_g, q_g, r_g) = \left(\frac{\partial w_g}{\partial y}, -\frac{\partial w_g}{\partial x}, \frac{\partial v_g}{\partial x} - \frac{\partial u_g}{\partial y} \right)$$

Thomasson,[4] in a work regarding the equations of motion for a rigid vehicle in a moving fluid, resumes the main results of different authors and explains the difficulties related to the application of the different sets of equations of motion that are used for vehicles operating in unsteady conditions or in presence of wind gradients. The aforementioned difficulties are related to the fact that the gust forces and moments terms also depend on time and space variations of fluid velocities components and the explicit expression of such terms is not always simple to obtain. Then he deduces, using the Lagrange equation method, the motion equations and provides suitable expression for the force and moment terms that occur on a vehicle immersed in a nonuniform stream.

The principal objective of this study is to provide a sound mathematical model for the analysis of the performance of ultralight vehicles flying in a nonuniform wind field. The equations of motion are written according to the Lagrange equation method, where the kinetic energy of the airstream is to be expressed in terms of relative velocity.[2]

This approach allows the microlift force contribution to the aircraft motion to be expressed accurately and possible performance improvements to be interpreted. In particular, following a preliminary discussion on the definition of microlift force, the equations of motion are formulated and the microlift coefficient C_{L_m} is determined as a function of the wind velocity gradient. After providing some details on the sailplane model and its aerodynamic characteristics, a parametric study of the influence of the microlift on the vehicle motion is presented. Finally, some applications of the method to maneuvers and piloting techniques of an ultralight aircraft flying in a wind gradient are discussed.

Microlift Force

When an aircraft in horizontal flight experiences a vertical gust, a mass of air about the aircraft is accelerated by the motion of the vehicle itself.[5] In this circumstance an additional force term $\boldsymbol{F}_m$, approximately perpendicular to flight velocity, appears in the motion equations. This term is a function of the local gradient of the wind velocity and is related to the virtual mass of the glider as

$$|\boldsymbol{F}_m| \approx M_A \frac{\partial w_g}{\partial s} V \tag{1}$$

where $(\partial w_g/\partial s)V$ is an appropriate value of the acceleration of the fluid mass. In a first approximation one could evaluate M_A as the mass contained in a cylinder with diameter equal to the mean wing chord and length equal to the wing span,[6] that is,

$$M_A \approx \rho(\pi/4)Sc \tag{2}$$

Equations (1) and (2) are obtained by assuming that the fluid flow is potential and the acceleration of the fluid mass about the aircraft is equal to $(\partial w_g/\partial s)V$. In this approximate context $\boldsymbol{F}_m$ could be defined as the microlift force.

A different way to explain the microlift effect, from Küssner,[7] is to express the portion of lift related to the gust gradient as a linear response of the time derivative of the angle of attack induced by the gradient $\partial w_g/\partial s$, that is,

$$|\boldsymbol{F}_m| = \int_0^t K(t,\tau)\dot{\alpha}(\tau)\,\mathrm{d}\tau = \int_0^t K(t,\tau)\frac{\partial w_g}{\partial s}\,\mathrm{d}\tau \tag{3}$$

where $K(t,\tau)$ is the impulsive response. If both $\partial w_g/\partial s$ and V are constant, $|\boldsymbol{F}_m|$ will be expressed as

$$|\boldsymbol{F}_m| = \frac{\partial w_g}{\partial s}\int_0^t K(t,\tau)\,\mathrm{d}\tau \tag{4}$$

where the integral, when computed over a sufficiently long time interval, is proportional to M_A.

For instance, an ultralight aircraft with $W = 900$ N, $S = 18$ m^2, and $c = 1.8$ m has a virtual mass of about 32 kg as shown by Jones.[5] Therefore, according to Eq. (1), this kind of aircraft in a vertical gust with a gradient $\partial w_g/\partial s = 0.2$ s^{-1} at a velocity of 30 m s^{-1} will experience a vertical force $|\boldsymbol{F}_m| \approx 200$ N that represents more than 20% of the vehicle weight.

Calculation Method

A method to calculate the aerodynamic forces that occur in flight, in the presence of a wind gradient, is now presented. To derive an accurate expression of the force responsible for the microlift phenomenon, an aircraft in a potential flow with a constant gradient of the wind velocity is considered. The expression of the kinetic energy of the stream in terms of apparent mass tensor $\boldsymbol{M}$ and relative velocity $\boldsymbol{v} - \boldsymbol{L}\boldsymbol{w}_g$ is[2]

$$T = \frac{1}{2}\rho\int_S \boldsymbol{\phi}\boldsymbol{n}\cdot\boldsymbol{v}\,\mathrm{d}S = \frac{1}{2}(\boldsymbol{v} - \boldsymbol{L}\boldsymbol{w}_g)\cdot\boldsymbol{M}(\boldsymbol{v} - \boldsymbol{L}\boldsymbol{w}_g) \tag{5}$$

where

$$\boldsymbol{L} = \begin{bmatrix} \cos\vartheta\cos\psi & \cos\vartheta\sin\psi & -\sin\vartheta \\ \sin\varphi\sin\vartheta\cos\psi - \cos\varphi\sin\psi & \sin\varphi\sin\vartheta\sin\psi + \cos\varphi\cos\psi & \sin\varphi\cos\vartheta \\ \cos\varphi\sin\vartheta\cos\psi + \sin\varphi\sin\psi & \cos\varphi\sin\vartheta\sin\psi - \sin\varphi\cos\psi & \cos\varphi\cos\vartheta \end{bmatrix}$$

In Eq. (5) the contribution to the kinetic energy of the terms depending on the angular velocity is neglected. Next, $\boldsymbol{M}$ expressed in body

axes is constant and does not depend on the angles of attack and sideslip.[2] The aerodynamic force $\boldsymbol{F}$ and moment $\boldsymbol{Q}$ on the aircraft are expressed using the Lagrange equations in the general form

$$\boldsymbol{F} = -\frac{\mathrm{d}}{\mathrm{d}t}\frac{\partial T}{\partial \boldsymbol{v}} - \boldsymbol{\omega} \times \frac{\partial T}{\partial \boldsymbol{v}} \tag{6}$$

$$\boldsymbol{Q} = -\boldsymbol{v} \times \frac{\partial T}{\partial \boldsymbol{v}} + \boldsymbol{r}_{\mathrm{AG}} \times \boldsymbol{F} \tag{7}$$

where $\boldsymbol{r}_{\mathrm{AG}}$ represents the position of the aerodynamic center with respect to c.g. Substituting Eq. (5) into Eq. (6) and taking into account the time variation of $\boldsymbol{L}$, one obtains

$$\boldsymbol{F} = -\big[\boldsymbol{M}\dot{\boldsymbol{v}} + \boldsymbol{\omega} \times \boldsymbol{M}(\boldsymbol{v} - \boldsymbol{L}\boldsymbol{w}_g) + \dot{\boldsymbol{M}}(\boldsymbol{v} - \boldsymbol{L}\boldsymbol{w}_g) + \boldsymbol{M}(\boldsymbol{\omega} \times \boldsymbol{L}\boldsymbol{w}_g) - \boldsymbol{M}\boldsymbol{L}\nabla\boldsymbol{w}_g\boldsymbol{L}^T\boldsymbol{v}\big] \tag{8}$$

The first term in Eq. (8), usually neglected in flight dynamics, represents the inertia force of the airflow, whereas the second and third ones are, respectively, the contribution of the rotary derivatives and the classical expression of the lift related to the circulation around the wing according to the Kutta–Joukowskij theorem. The latter term also includes the contribution of the induced drag.

Next, the fourth term in Eq. (8) represents the combined effects of angular velocity and wind velocity, and the fifth,

$$\hat{\boldsymbol{F}}_m = \boldsymbol{M}\boldsymbol{L}\nabla\boldsymbol{w}_g\boldsymbol{L}^T\boldsymbol{v} \tag{9}$$

is caused by the effects of both wind gradient and flight velocity. Although Eq. (9) shows that $\hat{\boldsymbol{F}}_m$ has an arbitrary direction depending upon $\boldsymbol{M}$, $\nabla\boldsymbol{w}_g$, $\boldsymbol{L}$, and $\boldsymbol{v}$, according to Ref. 7, the suction force on the wing leading edge transforms $\hat{\boldsymbol{F}}_m$ into a vector $\boldsymbol{F}_m$, called *microlift*, which has the same length of $\hat{\boldsymbol{F}}_m$, and it is perpendicular to the relative velocity, that is,

$$\boldsymbol{F}_m = \frac{\hat{\boldsymbol{F}}_m - (\hat{\boldsymbol{F}}_m \cdot \hat{\boldsymbol{v}})\hat{\boldsymbol{v}}}{|\hat{\boldsymbol{F}}_m - (\hat{\boldsymbol{F}}_m \cdot \hat{\boldsymbol{v}})\hat{\boldsymbol{v}}|}|\hat{\boldsymbol{F}}_m| \tag{10}$$

Equations (9) and (10), which yield the mathematical expression of microlift force, are consistent with the qualitative definition given in the Introduction.

As a further observation, Eq. (8) shows that $\boldsymbol{M}$ and $\dot{\boldsymbol{M}}$ represent the derivatives of the aerodynamic force $\boldsymbol{F} \equiv (X, Y, Z)$ with respect to the acceleration and velocity components, respectively. Therefore they can be expressed in terms of aerodynamic derivatives as

$$\boldsymbol{M} = \begin{bmatrix} -\frac{\partial X}{\partial \dot{u}} & -\frac{\partial X}{\partial \dot{v}} & -\frac{\partial X}{\partial \dot{w}} \\ -\frac{\partial Y}{\partial \dot{u}} & -\frac{\partial Y}{\partial \dot{v}} & -\frac{\partial Y}{\partial \dot{w}} \\ -\frac{\partial Z}{\partial \dot{u}} & -\frac{\partial Z}{\partial \dot{v}} & -\frac{\partial Z}{\partial \dot{w}} \end{bmatrix}$$

$$\dot{\boldsymbol{M}} = \begin{bmatrix} -\frac{\partial X}{\partial u} & -\frac{\partial X}{\partial v} & -\frac{\partial X}{\partial w} \\ -\frac{\partial Y}{\partial u} & -\frac{\partial Y}{\partial v} & -\frac{\partial Y}{\partial w} \\ -\frac{\partial Z}{\partial u} & -\frac{\partial Z}{\partial v} & -\frac{\partial Z}{\partial w} \end{bmatrix} \tag{11}$$

where one has

$$\frac{\partial X}{\partial \dot{v}} - \frac{\partial Y}{\partial \dot{u}} = \frac{\partial X}{\partial \dot{w}} - \frac{\partial Z}{\partial \dot{u}} = \frac{\partial Y}{\partial \dot{w}} - \frac{\partial Z}{\partial \dot{v}} = 0$$

as a result of the symmetry of $\boldsymbol{M}$.

In case of a variable wind gradient in inertial coordinates and in order to take into account the unsteady effect, in place of $\nabla\boldsymbol{w}_g$ a reduced wind gradient $\boldsymbol{G}$ obtained through the integration of a first-order differential equation that describes the time history of $\boldsymbol{G}$ as an evolution process toward $\nabla\boldsymbol{w}_g$ is used. The characteristic time of this process is $\mathcal{O}(c/V)$. Thus, the following equations are obtained:

$$\hat{\boldsymbol{F}}_m = \boldsymbol{M}\boldsymbol{L}\boldsymbol{G}\boldsymbol{L}^T\boldsymbol{v} \tag{12}$$

$$\dot{\boldsymbol{G}} = (\chi V/c)(\nabla\boldsymbol{w}_g - \boldsymbol{G}) \tag{13}$$

$$\boldsymbol{F} = -[\boldsymbol{M}\dot{\boldsymbol{v}} + \boldsymbol{\omega} \times \boldsymbol{M}(\boldsymbol{v} - \boldsymbol{L}\boldsymbol{w}_g) + \dot{\boldsymbol{M}}(\boldsymbol{v} - \boldsymbol{L}\boldsymbol{w}_g) + \boldsymbol{M}(\boldsymbol{\omega} \times \boldsymbol{L}\boldsymbol{w}_g) + \boldsymbol{F}_m] \tag{14}$$

where $\chi = \mathcal{O}(1)$ is a suitable constant to be identified through flight data or numerical computation of the flowfield.

As for the initial condition for $\boldsymbol{G}$ in Eq. (13), in all of the calculations it is $\boldsymbol{G}(t=0) = 0$.

In Eq. (8) it is possible to recognize some of the force terms presented in Refs. 2 and 4. In particular a correspondence between what here is called microlift and what in Ref. 4 is the term depending on the wind gradient is remarked. The force term responsible for lift and induced drag in Eq. (8) is not considered in Refs. 2 and 4 because only nonlifting bodies are dealt with in Ref. 2, whereas lift and induced drag are included in the external force terms in Ref. 4.

As for the expression of $\boldsymbol{Q}$ in Eq. (7), the first term, which is the same obtained by Lamb[2] for $\boldsymbol{\omega} = 0$, represents the contribution of the apparent mass tensor. The second one, not considered in Ref. 2, gives the moment of $\boldsymbol{F}$ with respect to the aircraft c.g.

At this point the motion equations for a rigid aircraft are written as[8]

$$m(\dot{\boldsymbol{v}} + \boldsymbol{\omega} \times \boldsymbol{v}) = \boldsymbol{F}^e, \qquad \boldsymbol{J}\dot{\boldsymbol{\omega}} + \boldsymbol{\omega} \times \boldsymbol{J}\boldsymbol{\omega} = \boldsymbol{Q}^e$$
$$\dot{\boldsymbol{r}} = \boldsymbol{L}^T\boldsymbol{v}, \qquad \dot{\boldsymbol{\Phi}} = \boldsymbol{R}^{-1}\boldsymbol{\omega} \tag{15}$$

with $\boldsymbol{F}^e = m\boldsymbol{L}\boldsymbol{g} + \boldsymbol{F} + \boldsymbol{F}_v$ and $\boldsymbol{Q}^e = \boldsymbol{Q}$, where $m\boldsymbol{L}\boldsymbol{g}$ is the weight force expressed in body axes and $\boldsymbol{F}_v$ which plays the role of a purely dissipative action, is the aerodynamic viscous force. Next, $\boldsymbol{R}^{-1}$ is the transformation matrix from angular velocity to time derivative of the Euler's angles:

$$\boldsymbol{R}^{-1} = \begin{bmatrix} 0 & \cos\varphi & -\sin\varphi \\ 1 & \sin\varphi\tan\vartheta & \cos\varphi\tan\vartheta \\ 0 & \sin\varphi\sec\vartheta & \cos\varphi\sec\vartheta \end{bmatrix}$$

Substituting in place of $\boldsymbol{F}$ its expression given by Eq. (14) and taking into account Eqs. (10), (12), and (13), one obtains the following augmented system that allows, in the general case, the evaluation of unsteady effects caused by an abrupt variation of the gust velocity profile:

$$\boldsymbol{M}_T\dot{\boldsymbol{v}} + \boldsymbol{\omega} \times \boldsymbol{M}_T\boldsymbol{v} = \boldsymbol{F}_0 + \boldsymbol{F}_m + m\boldsymbol{L}\boldsymbol{g}, \qquad \boldsymbol{J}\dot{\boldsymbol{\omega}} + \boldsymbol{\omega} \times \boldsymbol{J}\boldsymbol{\omega} = \boldsymbol{Q}^e$$
$$\dot{\boldsymbol{G}} = \frac{\chi V}{c}(\nabla\boldsymbol{w}_g - \boldsymbol{G}), \qquad \dot{\boldsymbol{r}} = \boldsymbol{L}^T\boldsymbol{v}, \qquad \dot{\boldsymbol{\Phi}} = \boldsymbol{R}^{-1}\boldsymbol{\omega}$$
$$\hat{\boldsymbol{F}}_m = \boldsymbol{M}\boldsymbol{L}\boldsymbol{G}\boldsymbol{L}^T\boldsymbol{v}, \qquad \boldsymbol{F}_m = \frac{\hat{\boldsymbol{F}}_m - (\hat{\boldsymbol{F}}_m \cdot \hat{\boldsymbol{v}})\hat{\boldsymbol{v}}}{|\hat{\boldsymbol{F}}_m - (\hat{\boldsymbol{F}}_m \cdot \hat{\boldsymbol{v}})\hat{\boldsymbol{v}}|}|\hat{\boldsymbol{F}}_m| \tag{16}$$

where $\boldsymbol{M}_T = \boldsymbol{I}m + \boldsymbol{M}$, $\boldsymbol{I}$ is the unit tensor, and $\boldsymbol{F}_0$ gives

$$\boldsymbol{F}_0 = \boldsymbol{\omega} \times \boldsymbol{M}\boldsymbol{L}\boldsymbol{w}_g - \boldsymbol{M}(\boldsymbol{\omega} \times \boldsymbol{L}\boldsymbol{w}_g) + [-\dot{\boldsymbol{M}}(\boldsymbol{v} - \boldsymbol{L}\boldsymbol{w}_g) + \boldsymbol{F}_v] \tag{17}$$

The term within square brackets represents the aerodynamic force depending on α, β, and V, and, in what follows, it is supposed that it can be expressed, in usual fashion, through the aerodynamic force coefficients.

As shown in Eqs. (16), the presence of the microlift and of all the other terms that depend on $\boldsymbol{M}$ modifies the equations of motion of the aircraft, and the variations can be very significant for ultralight vehicles.

At this point it is important to note some relevant consequences on the motion of the aircraft related to the presence, in Eqs. (16), of additional force terms. First, the $\boldsymbol{M}_T\dot{\boldsymbol{v}}$ term is a linear transformation of the time derivative of the velocity that, in general, is not parallel

to $\dot{\boldsymbol{v}}$. Furthermore, not all of the additional terms depend on $\boldsymbol{w}_g$ as for instance $\boldsymbol{M}\dot{\boldsymbol{v}}$ and $\boldsymbol{\omega} \times \boldsymbol{M}\boldsymbol{v}$, and, therefore, they can play a role also in the absence of wind. In particular, if a motion in calm air is considered the work of the external force is equal to the variation of $E + \frac{1}{2}\boldsymbol{v}\boldsymbol{M}\boldsymbol{v}$, which is the sum of the mechanical energy of the aircraft and the kinetic energy of the flow. As a consequence, the aircraft motion can be affected, to some extent, by the conversion of the latter form of energy into vehicle mechanical energy and vice versa. This effect is usually neglected in classical flight dynamics.

To study the influence of the microlift on the performances of an ultralight sailplane, an aircraft in steady flight condition in the presence of a constant vertical wind gradient is considered. To simplify such an approach, the attitude of the aircraft is given as $\varphi = \vartheta = \psi = 0$ so that $\boldsymbol{L} = \boldsymbol{I}$, and the gust velocity is zero in the aircraft c.g. In the model this corresponds to $w_g = 0$. Therefore, the microlift can be expressed as

$$\boldsymbol{F}_m = \boldsymbol{M}\nabla\boldsymbol{w}_g\boldsymbol{v} \tag{18}$$

For an aircraft configuration the more sizeable contribution to $\boldsymbol{F}_m$ is given by $M_{33} \equiv -\partial Z/\partial \dot{w}$ while the other elements of the apparent mass matrix have usually minor influence. Furthermore,

$$M_{12} \equiv -\frac{\partial X}{\partial \dot{v}} = M_{23} \equiv -\frac{\partial Y}{\partial \dot{w}} = 0$$

because in most cases (x_B, z_B) is a symmetry plane. Hence, in this approximate framework $\boldsymbol{M}$ is

$$\boldsymbol{M} = \begin{bmatrix} 0 & 0 & 0 \\ 0 & 0 & 0 \\ 0 & 0 & M_{33} \end{bmatrix} \tag{19}$$

As for the wind gradient, it is supposed that w_g which can change in the horizontal plane (x, y) is only

$$\nabla\boldsymbol{w}_g = \begin{bmatrix} 0 & 0 & 0 \\ 0 & 0 & 0 \\ \dfrac{\partial w_g}{\partial x} & \dfrac{\partial w_g}{\partial y} & 0 \end{bmatrix} \tag{20}$$

Introducing Eqs. (19) and (20) into Eq. (18) and taking into account that $\boldsymbol{v} = V(\cos\alpha\cos\beta, \sin\beta, \sin\alpha\cos\beta)$, the microlift coefficient becomes

$$C_{L_m} = \frac{2|\boldsymbol{F}_m|}{\rho V^2 S} = \frac{2M_{33}}{\rho S V}\left(\frac{\partial w_g}{\partial x}\cos\alpha\cos\beta + \frac{\partial w_g}{\partial y}\sin\beta\right) \tag{21}$$

C_{L_m} is proportional to the inverse of flight speed; therefore, its influence is relevant at low velocities. Equation (21) demonstrates that, in the presence of a vertical wind gradient, it is possible to obtain microlift force in different ways depending on $\partial w_g/\partial x$, $\partial w_g/\partial y$, and β, as illustrated in Fig. 1. In particular, in order to have microlift, as shown in Figs. 1a and 1b, it is sufficient to fly in such a way that the flight path intersects the iso-w_g lines (dashed) with a nonzero angle. Furthermore, from Eq. (21) for a given angle of attack the maximum value of microlift coefficient is achieved for

$$\beta[(C_{L_m})_{\max}] = \arctan\frac{\partial w_g/\partial y}{(\partial w_g/\partial x)\cos\alpha} \tag{22}$$

In Figs. 1c and 1d the two flight conditions at $\beta \neq 0$ and $\beta = 0$ are presented, respectively, both corresponding to the development of a maximum value for microlift coefficient. In both cases the maximum value for C_{L_m} is reached when the angle between velocity vector and iso-w_g lines is about $\pi/2$. Furthermore, with $\partial w_g/\partial x = 0$ in Eq. (22) then the maximum microlift coefficient is achieved for $|\beta| = \pi/2$. These effects will be discussed in more detail in the next section, when the influence of the wind gradient on the trim conditions is analyzed.

Minor effects of microlift force are observed if all of the elements of the apparent mass tensor are accounted for. In the case where $M_{13} \equiv -\partial X/\partial \dot{w} \neq 0$, being $|M_{13}| \ll |M_{33}|$, the increase of the microlift coefficient is approximatively given by $(M_{13}/\rho S V)(M_{13}/M_{33})[(\partial w_g/\partial x)\cos\alpha\cos\beta + (\partial w_g/\partial y)\sin\beta]$, which is much lower than C_{L_m} as expressed in Eq. (21).

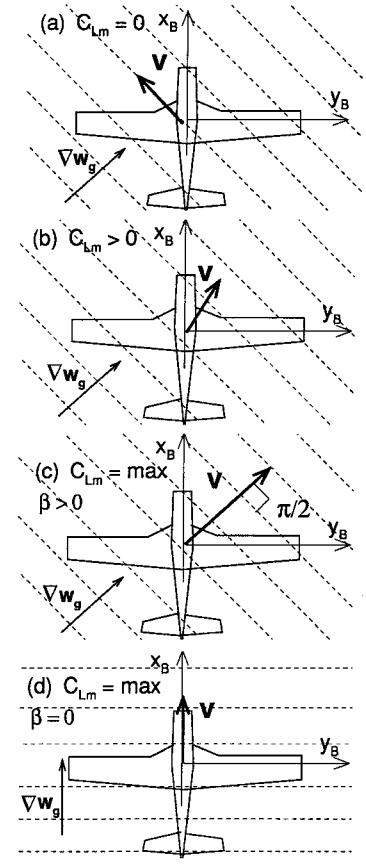

Fig. 1 Influence of the wind gradient on microlift.

Next, in order to study the unsteady effects on the microlift, the case of a vertical gust with a step velocity variation in the (x_B, z_B) plane is considered. In this case the wind gradient has an impulse $w_g\delta(s, \bar{s})$, and all of the coefficients G_{ij} in Eq. (13) are zero but G_{31}. Hence,

$$\dot{G}_{31} = (\chi V/c)[\delta(s, \bar{s})w_g - G_{31}] \tag{23}$$

By integrating Eq. (23) between $\bar{s} - \varepsilon$ and $\bar{s} + \varepsilon$, for very small ε one obtains a relationship that relates the reduced wind gradient variation to w_g:

$$\Delta G_{31} = \chi w_g/c \tag{24}$$

Then, introducing Eq. (24) into Eq. (12) and taking into account Eq. (2) the expression of microlift variation is

$$\Delta|\boldsymbol{F}_m| \approx M_A \Delta G_{31} V = M_A(\chi w_g V/c) \approx \rho\pi S\chi w_g V/4 \tag{25}$$

that, in terms of C_{L_m}, becomes

$$\Delta C_{L_m} = \chi(\pi/2)(w_g/V) \tag{26}$$

so as to recover the classic result[6] for the C_L increase caused by a sharp edge gust

$$\Delta C_L \approx C_{L_\alpha}(w_g/V) \tag{27}$$

Therefore, comparison between Eqs. (26) and (27) confirms that $\chi \approx (2/\pi)C_{L_\alpha}$ is $\mathcal{O}(1)$.

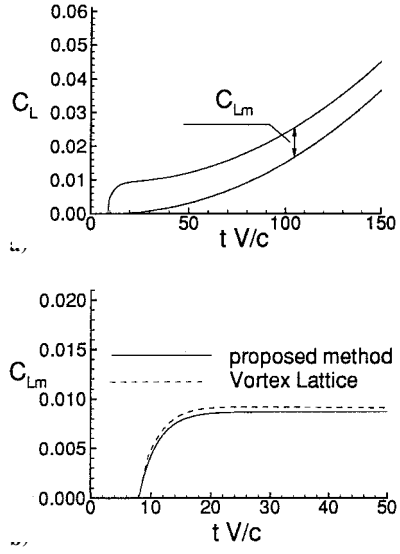

Fig. 2 Time histories of the lift coefficients.

Validation of the Method

To validate the proposed method, the lift coefficient of a linearly tapered wing, having aspect ratio and taper ratio equal to 27.59 and 0.54, respectively, is computed, as a function of time, by an unsteady vortex-lattice code, where the effects of a longitudinal wind gradient $\partial w_g/\partial s$ are accounted for. In particular, a linear distribution of the vertical velocity in two cases is evaluated.

In the first one the inertial acceleration of the flow, expressed through the $\partial\phi/\partial t$ term of the Bernoulli's equation, is accounted for, and the normal velocity on the wing surface is specified as

$$\boldsymbol{n}(\boldsymbol{x})\cdot\boldsymbol{v}_w(\boldsymbol{x}) = \boldsymbol{n}\cdot[\boldsymbol{v}+\boldsymbol{w}_g(\boldsymbol{x}_G)+\nabla\boldsymbol{w}_g(\boldsymbol{x}-\boldsymbol{x}_G)] \qquad (28)$$

where $\boldsymbol{v}_w$ represents the local velocity at the generic point $\boldsymbol{x}$ of the wing, $\boldsymbol{x}_G$ is the c.g. position, and $\boldsymbol{v}$, which is assumed constant, is the wing velocity.

In the second situation the pressure field on the wing is calculated for steady-state conditions, and the wind effects are represented through the following boundary condition on the wing surface:

$$\boldsymbol{n}(\boldsymbol{x})\cdot\boldsymbol{v}_w(\boldsymbol{x}) = \boldsymbol{n}\cdot[\boldsymbol{v}+\boldsymbol{w}_g(\boldsymbol{x}_G)] \qquad (29)$$

According to the definition of microlift force, the microlift coefficient can be evaluated as the difference between the lift coefficient calculated using Eqs. (28) and (29) respectively because in the latter case unsteady effects are neglected, the wind gradient is not considered, and, as a result, the aerodynamic force only depends on the instantaneous variation of the angle of attack.

The results of the analysis, obtained for $(\partial w_g/\partial x_B)(c/V) = 0.005$, are presented in Fig. 2a for both the considered cases. The difference between the two curves gives the microlift coefficient. Figure 2b shows that the values of C_{L_m} obtained from Eqs. (10), (12), and (13) with $\chi = (2/\pi)C_{L_\alpha}$ and the vortex lattice method are in good agreement and that the relative differences between the two values are lower than 6%. This demonstrates that the proposed method provides accurate time histories of microlift coefficient.

Results and Discussion

Consider a model of the $ASH-26E$ sailplane sketched in Fig. 3, the design parameters of which are $b = 18.0$ m, $S = 11.7$ m^2, $l = 13.5$ m, $AR = 27.69$, high horizontal tail. The wing loading is assumed equal to 100 N m^{-2}. The aerodynamic characteristics of the sailplane were estimated by the boundary element code VSAERO by Analytical Methods, Inc.,[9] in the range, for the aerodynamic angles, $-25 \le \alpha \le 25$, $-15 \le \beta \le 15$. Table 1 reports the computed aerodynamic coefficients in body axes as functions of the aerodynamic

Table 1 Aerodynamic coefficients of the sailplane vs α and β

β, deg; α, deg	0	5	10	15
		a) $C_x \times 10$		
−25	4.59	4.57	4.49	4.36
−20	2.69	2.68	2.64	2.58
−15	1.22	1.22	1.21	1.20
−10	0.24	0.25	0.26	0.29
−5	−0.23	−0.22	−0.19	−0.15
0	−0.13	−0.12	−0.10	−0.05
5	0.51	0.51	0.52	0.55
10	1.64	1.63	1.61	1.59
15	3.26	3.24	3.19	3.11
20	5.29	5.26	5.16	5.01
25	7.69	7.64	7.49	7.25
		b) $C_l \times 100$		
−25	0.00	0.01	0.06	0.11
−20	0.00	−0.08	−0.14	−0.19
−15	0.00	−0.17	−0.31	−0.45
−10	0.00	−0.26	−0.50	−0.73
−5	0.00	−0.35	−0.68	−0.98
0	0.00	−0.44	−0.86	−1.26
5	0.00	−0.51	−1.01	−1.48
10	0.00	−0.58	−1.16	−1.70
15	0.00	−0.66	−1.30	−1.88
20	0.00	−0.71	−1.43	−2.07
25	0.00	−0.79	−1.50	−2.26
		c) $C_y \times 10$		
−25	0.00	−0.23	−0.42	−0.58
−20	0.00	−0.22	−0.43	−0.60
−15	0.00	−0.22	−0.42	−0.59
−10	0.00	−0.21	−0.40	−0.59
−5	0.00	−0.22	−0.40	−0.59
0	0.00	−0.20	−0.38	−0.57
5	0.00	−0.19	−0.37	−0.55
10	0.00	−0.17	−0.34	−0.52
15	0.00	−0.15	−0.33	−0.48
20	0.00	−0.14	−0.30	−0.44
25	0.00	−0.14	−0.30	−0.46
		d) C_m		
−25	−0.22	−0.23	−0.23	−0.24
−20	−0.03	−0.03	−0.04	−0.05
−15	0.12	0.12	0.11	0.09
−10	0.22	0.22	0.21	0.19
−5	0.25	0.25	0.23	0.21
0	0.21	0.20	0.19	0.18
5	0.11	0.11	0.09	0.08
10	−0.02	−0.02	−0.03	−0.04
15	−0.18	−0.18	−0.19	−0.20
20	−0.42	−0.41	−0.41	−0.41
25	−0.69	−0.68	−0.68	−0.67
		e) C_z		
−25	1.74	1.73	1.69	1.63
−20	1.36	1.35	1.32	1.27
−15	0.91	0.90	0.88	0.85
−10	0.41	0.41	0.40	0.39
−5	−0.11	−0.11	−0.11	−0.10
0	−0.66	−0.66	−0.64	−0.62
5	−1.20	−1.20	−1.17	−1.12
10	−1.71	−1.70	−1.66	−1.60
15	−2.19	−2.17	−2.12	−2.04
20	−2.60	−2.58	−2.52	−2.43
25	−2.94	−2.92	−2.86	−2.75
		f) $C_n \times 100$		
−25	0.00	0.48	0.86	1.20
−20	0.00	0.45	0.84	1.16
−15	0.00	0.44	0.80	1.12
−10	0.00	0.41	0.74	1.09
−5	0.00	0.39	0.71	1.06
0	0.00	0.34	0.66	0.98
5	0.00	0.32	0.62	0.92
10	0.00	0.27	0.55	0.83
15	0.00	0.23	0.49	0.73
20	0.00	0.20	0.42	0.64
25	0.00	0.16	0.36	0.55

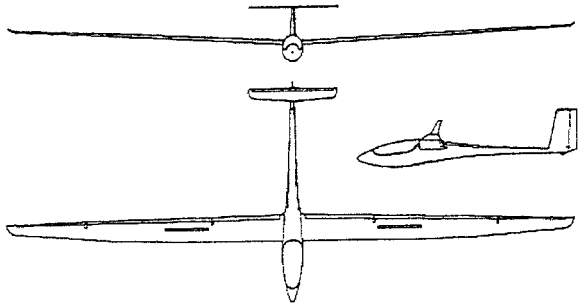

Fig. 3 ASH-26E sailplane.

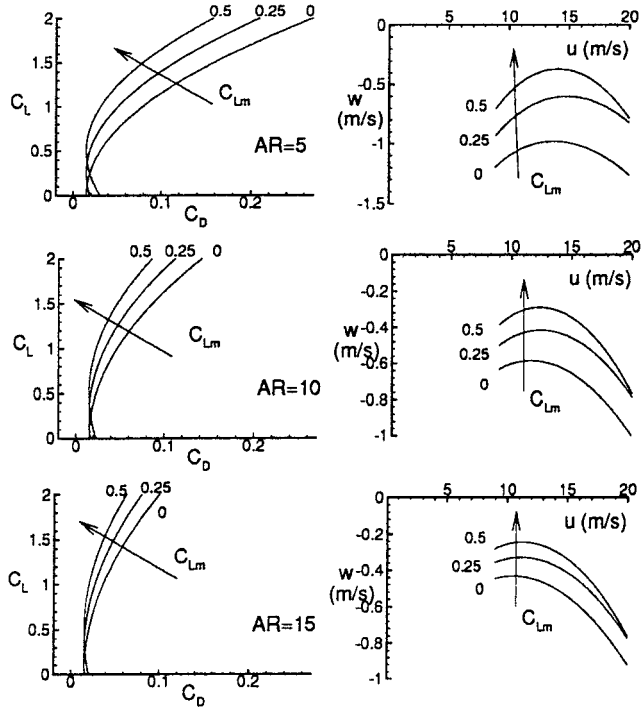

Fig. 4 Influence of microlift on gliding flight.

angles. The expressions of the incremental force and moment coefficients caused by the control angles are

$$\Delta C_x = -0.8829\times 10^{-5}\delta_e^2 - 0.1705\times 10^{-4}\delta_r^2 - 0.3448\times 10^{-4}\delta_e^2$$

$$\Delta C_y = 0.2976\times 10^{-2}\delta_r$$

$$\Delta C_z = -0.4025\times 10^{-2}\delta_e - 0.3004\times 10^{-5}\delta_r^2 + 0.6076\times 10^{-4}\delta_a^2$$

$$\Delta C_l = -0.5227\times 10^{-2}\delta_a + 0.1485\times 10^{-3}\delta_r$$

$$\Delta C_m = -0.3422\times 10^{-1}\delta_e + 0.4824\times 10^{-4}\delta_a^2 - 0.1731\times 10^{-5}\delta_r^2$$

$$\Delta C_n = -0.1611\times 10^{-3}\delta_a - 0.7259\times 10^{-3}\delta_r \qquad (30)$$

In what follows, in order to analyze the influence of the microlift some results regarding the flight of an ultralight sailplane into a severe wind gradient are presented. To this end, it will be considered the effect of different values of the aspect ratio $\mathcal{R}_N$ on drag coefficient according to

$$C_D(\mathcal{R}_N) - C_D(\mathcal{R}) = (1/\mathcal{R}_N - 1/\mathcal{R})\left(C_L^2/\pi e\right)$$

where $\mathcal{R}_N$ is the variable value of the aspect ratio and e is the Oswald factor, which is held constant and equal to $(1/\pi\mathcal{R})(\mathrm{d}C_L^2/\mathrm{d}C_D)$, computed for $\alpha = 0$, $\beta = 0$. Consequently, different aerodynamic force coefficients in body axes are obtained.

As a preliminary result, Fig. 4 shows the influence of the microlift on the drag polar and the odograph of the gliding flight for different

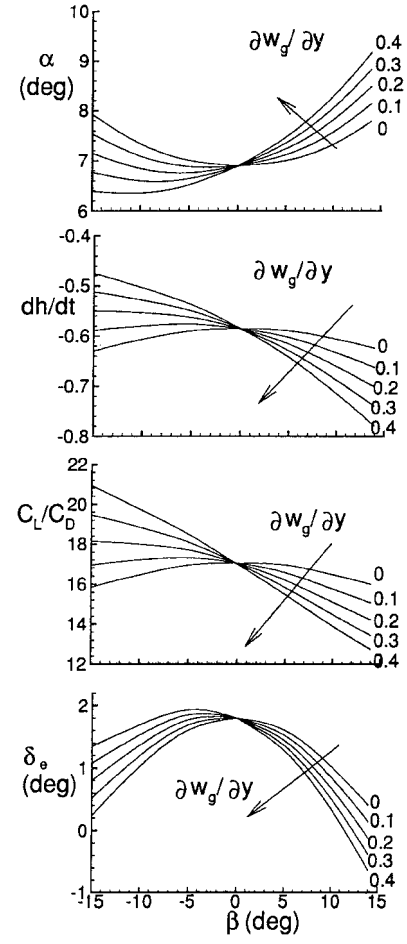

Fig. 5 Influence of wind gradient on glider trim.

values of the aspect ratio. In the diagrams each curve is referred to a given value of the microlift coefficient. In this case $W = 1000$ N, $S = 10$ m^2, and three values of the aspect ratio are $\mathcal{R} = 5$, 10, and 15.

The maximum value of C_{L_m} is taken approximately equal to 0.5 according to

$$C_{L_m} \approx \frac{M_A(\partial w_g/\partial x_B)V}{\frac{1}{2}\rho S V^2} \approx \frac{\pi}{2}c\frac{\partial w_g}{\partial x_B}\frac{1}{V} = \mathcal{O}(1)$$

where $\partial w_g/\partial x_B = 1$, $V = 10$ m s^{-1}, and $c = 1$ m. These values are assumed on the basis of typical conditions in which the microlift plays a role. A significant influence of C_{L_m} can be observed in the figure. In particular, the efficiency increases in any case by at least 40% with respect to the case of zero wind gradient, causing a significant reduction of the vertical velocities, which, in turn, improves the gliding performance. Such effects are particularly intense for ultralight aircraft with low aspect ratio. Figure 5 shows, in trim conditions, the variations of angle of attack, sink rate, aerodynamic efficiency, and the elevator angle vs sideslip angle for different values of the lateral wind gradient $\partial w_g/\partial y_B$. Here, y_B has the same direction of wing span. The trim conditions are obtained for flight velocity of 10 m s^{-1} at an altitude of 1000 m. It is supposed that the sailplane flies into a gust with linear velocity distribution $w_g(y_B)$ having zero value in the c.g. In the model this corresponds to assuming the wind velocity equal to zero. The wind gradient $\partial w_g/\partial y_B$ is variable from 0 to 0.5 s^{-1}. Furthermore, according to Eq. (19), it is assumed that the apparent mass matrix has all of the coefficients equal to zero but M_{33}, which is put equal to $m/2$.

The plots in Fig. 5 show that the wind gradient can substantially modify the aerodynamic coefficients, causing relevant variations of the aerodynamic efficiency and, therefore, of the sink rate.

The best values of aerodynamic efficiency and sink rate, for the required trim condition, are realized for nonzero values of the sideslip

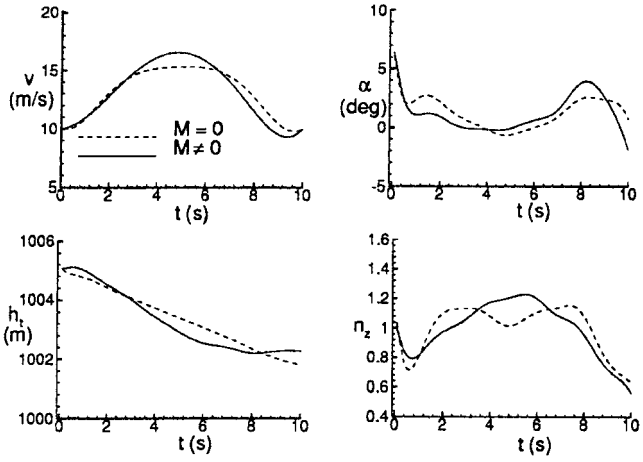

Fig. 6 Case 1: Influence of apparent mass on the sailplane motion in calm air.

angle. This means that the efficiency increase caused by microlift is greater than its reduction caused by a nonsymmetric flight condition. Ultralight sailplane pilots during some ascent maneuvers in the presence of a wind gradient find it more convenient to fly at nonzero sideslip angle.

A few simulations of vehicle motion to show the main effects related to both microlift and apparent mass are evaluated. To apply the method presented in the preceding section, the analysis will proceed from a simple maneuver to more complex ones. The objective in all of the simulations is to maximize the final altitude of the glider, where the control laws for δ_e, δ_a, and δ_r are determined by a constrained optimization method.[10] The trajectory optimization problem is formulated by a time discretization of the control laws, where the control angles are evaluated at 10 time locations. A continuous variation of δ_e, δ_a, and δ_r is obtained by spline interpolation.

Equations (16) are used as motion equations, and the contribution of the three control angles to the aerodynamic forces and moments is taken into account through incremental force and moment coefficients as reported in Eqs. (30).

To study the influence on the sailplane motion of the already cited additional force terms in Eqs. (16) and (17) that do not depend on the wind, the first maneuver takes place in the vertical plane and in calm air. The sailplane is initially in level flight at equilibrium speed $V = 10\,\mathrm{m\,s^{-1}}$ and altitude $h = 1000\,\mathrm{m}$. The maneuver duration is assigned equal to 10 s, and, as a final condition, the velocity is kept equal to 10 m s^{-1}. Figure 6 shows the time histories of some significant states and load factor, computed for $\boldsymbol{M} = 0$ (dashed lines) and $\boldsymbol{M} \neq 0$ (continuous line) with $M_{11} = M_{22} = M_{ij} = 0$, for $i \neq j$, and $M_{33}/m = 1$. The differences between the two solutions are evident as far as h_t and n_z are concerned. In particular, in the case of $\boldsymbol{M} \neq 0$ the slope of $h_t(t)$ is greater than zero at certain values of t. This circumstance is caused by the conversion of the flow energy into mechanical energy of the aircraft.

The second maneuver is three-dimensional, and the glider intersects a vertical gust, the velocity distribution of which is $w_g = A_g \sin^2(\pi x/H)$ for $0 \leq x \leq 60$ and $w_g = 0$ elsewhere, with $A_g = 5$ m s^{-1} and $H = 60$ m. At the initial time the sailplane is at the equilibrium speed $V = 10$ m s^{-1} with $h = 1000$ m and $\psi = 0$ out of the gust region. It must perform a maneuver lasting 10 s so as to align its longitudinal axis to the axis of the gust front. The prescribed final condition is defined as $V = 10$ m s^{-1}, $\beta = \phi = p = q = r = 0$, and $\psi = 90$ deg. The results are shown in Fig. 7, where again the continuous and dashed lines refer to $\boldsymbol{M} \neq 0$ and $\boldsymbol{M} = 0$, respectively. Some significant differences regarding V, δ_e, and α occur.

During the maneuver, the sailplane increases its energy height under the action of the vertical gust (Fig. 7e). The trajectories in the horizontal plane (x, y) (Fig. 7f) show how the positions of the aircraft are related to the gust velocity profile. In both cases the aircraft position at the end of the maneuver will be very close to the region where the gust speed reaches its maximum value. Higher

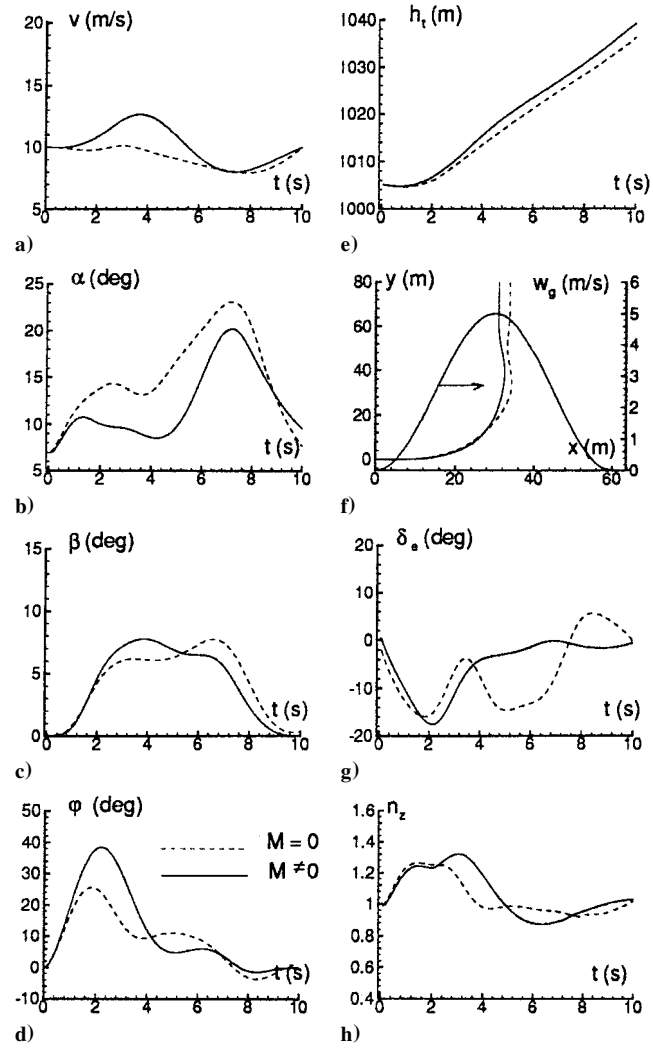

Fig. 7 Case 2: Three-dimensional maneuver in the presence of wind.

values of the roll angle (Fig. 7d) are obtained for $\boldsymbol{M} \neq 0$ because of the higher speed and the inertial effects of the virtual mass. The angle of attack (Fig. 7b) is significantly lower than those calculated for $\boldsymbol{M} = 0$ because of microlift effects, and, as a result, a different δ_e law is obtained. Furthermore, in the case of $\boldsymbol{M} \neq 0$ the average speed results greater than the one for $\boldsymbol{M} = 0$. This is because of the microlift force component in the direction of $\boldsymbol{v}$. The greater distance realized for $\boldsymbol{M} \neq 0$ allows the sailplane to complete the maneuver with a greater ratio between range and altitude variation. To maximize the final height, the pilot should adopt different control techniques in terms of elevator angle and flight speed. In this case the microlift effects produce a 13% improvement of the final altitude.

In the third case, shown in Fig. 8, the glider realizes a three-dimensional maneuver where vertical gust front is crossed. The velocity distribution is $w_g = A_g \sin^2(\pi y/H)$ for $0 \leq y \leq 60$, and $w_g = 0$ elsewhere, with $A_g = 5$ m s^{-1} and $H = 60$ m. At $t = 0$ the sailplane is in steady flight with $V = 10$ m s^{-1} at $h = 1000$ m out of the gust region. At the end of a 10-s maneuver, the longitudinal axis is to be parallel to the axis of the gust front. The assigned final conditions are $V = 10\,\mathrm{m\,s^{-1}}$, $\beta = \phi = \psi = p = q = r = 0$. Observe, in both cases, that the sailplane, under the influence of the vertical gust, increases its energy height (Fig. 8e). Relevant variations in the time histories of states and controls are apparent. This is true, in particular, for flight velocity (Fig. 8a) and angle of attack (Fig. 8b).

The computed angles of attack, at any time, take lower values for $\boldsymbol{M} \neq 0$. Such a result is directly connected to the microlift force, which acts to increase the total lift because of nonzero values of sideslip angle. The higher values of speed obtained for $\boldsymbol{M} \neq 0$ are the consequence of a nonnegligible positive microlift component in

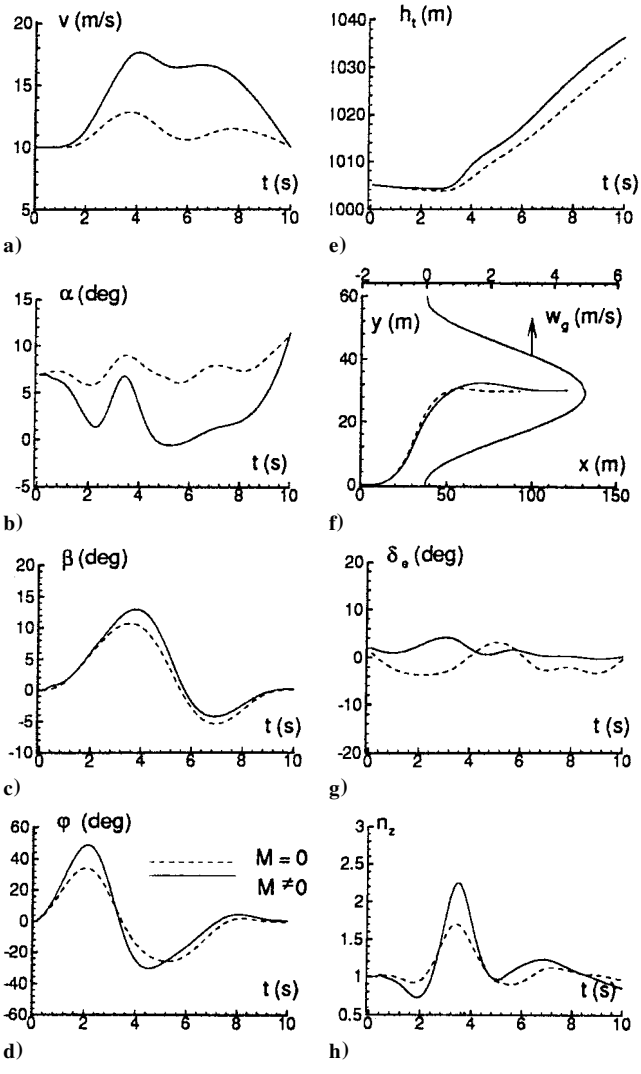

Fig. 8 Case 3: Three-dimensional maneuver in the presence of wind.

v direction. This, as shown in Fig. 8, allows the sailplane to have an increased range. Also, in the plot of the trajectories in the horizontal plane (x, y) (Fig. 8f) the final position of the vehicle is very close to the region where the gust speed is maximum. The altitude gain obtained through microlift effect is equal to approximately 20%.

In the reported simulations the presence of the apparent mass tensor in the equations of motion produces two opposite effects on the aircraft motion. On one hand, $\boldsymbol{M}$ tends to decrease the accelerations because it contributes to increase the mass of the physical system. On the other hand, the microlift term increases the lift coefficient, which tends, in turn, to increase the acceleration and then the load factor. In the case of a conventional aircraft with a relatively high wing loading, these effects are hidden by the low value of the M_A/m ratio. For an ultralight aircraft it is observed that $M_A/m = \mathcal{O}(1)$, and, therefore, both the aforementioned effects are significant.

Conclusions

In this study Lagrange equations and the apparent mass concept are used to express the microlift force developed by a ultralight sailplane soaring in a wind gradient.

Comparison with an unsteady vortex lattice method shows that the proposed method provides accurate results when the aerodynamic force developed by a wing in a nonuniform flow is calculated.

The results relative to the trim calculation and to the optimized simulations show that the consideration of microlift force in terms of apparent mass and wind gradient allows us to explain the improvement of gliding performance observed for low wing-loading sailplanes. Both microlift force and the other apparent-mass terms can significantly modify the aircraft behavior forcing the pilot to adopt nonconventional piloting techniques (microlift technique).

Therefore, whereas in conventional soaring technique a sailplane flying at a relatively high velocity through the vertical gust region steadily increases its altitude, the microlift technique prescribes a low flight speed through narrow regions where the wind velocity is not constant. Such a low speed is needed to increase the effect of microlift with respect to conventional lift force. Furthermore, in comparison with the ultralight vehicle a conventional sailplane cannot fly slow enough to take advantage of the microlift effect, even though a microlift force is always developed.

Because of its dependence on the wind gradient, the microlift force will result in a fleeting and rapidly changing force. Hence, the pilot, in order to use the microlift technique, must act on the controls, depending on wind gradient characteristics, that is direction and length, to realize timely variations of velocity and heading.

A final conclusion concerns the main limitation of the proposed method. As for the model of the microlift force, the results are valid under the assumption of potential flow about the aircraft. Also, in all of the calculations the influence of the virtual masses on the sailplane moments was neglected so that the possible effects on the attitude motion of the aircraft were not accounted for.

Acknowledgments

The author would like to thank Guido de Matteis for his helpful suggestions. This work was partially supported by Italian Ministry of University.

References

[1] Stojkovic B., "Semi-Dynamic Thermalling," *Technical Soaring*, Vol. 12, No. 1, 1988, pp. 10–14.

[2] Lamb, H., "On the Motion of Solids Through a Liquid," *Hydrodynamics*, 6th ed., Dover, New York, 1945, pp. 160–201.

[3] Etkin, B., "The Turbulent Wind and Its Effect on Flight," University of Toronto, *Institute for Aerospace Studies Review*, Vol. 44, 1980.

[4] Thomasson, P. G., "Equations of Motion of a Vehicle in a Moving Fluid," *Journal of Aircraft*, Vol. 37, No. 4, 2000, pp. 630–639.

[5] Jones, R. T., "Dynamics of Ultralight Aircraft-Motion in Vertical Gusts," NASA TM X-73228, April 1977, pp. 1–12.

[6] von Karman, Th., and Sears, W. R., "Airfoil Theory for Non-Uniform Motion," *Journal of Aeronautical Sciences*, Vol. 5, No. 1, Aug. 1938, pp. 379–390.

[7] Küssner, H. G., "Untersuchung del Bewegung einer Platte beim Eintritt in eine Strahlgrenze," *Luftfahrtforschung*, Bd 13, 1936, p. 425.

[8] Etkin, B., *Dynamics of Atmospheric Flight*, Wiley, New York, 1972, pp. 104, 152.

[9] *VSAERO User's Manual*, Rev. E5, Analytical Methods, Inc., April 1994, pp. 1–52.

[10] Polak, E., *Computational Methods in Optimization*, Academic Press, New York, 1971, pp. 56–68.